PHS3350 Final Report: Heavy-Flavour Baryons at the Large Hadron Collider

Claire Bergman
Supervisor: Peter Skands
Co-supervisor: Javira Altmann

September 2024

Abstract

Recent studies have shown that a QCD colour reconnection model incorporating string junctions can effectively describe heavy-flavour baryon production ratios, particularly for Λ_c^+/D^0. Despite these advancements, significant discrepancies emerge at low transverse momentum ($p_\perp$) in the Λ_b^0/B^0 ratio, where the model exhibits limitations in capturing the observed LHC data. This suggests that additional mechanisms or modifications may be needed to reflect the distinct production dynamics of Λ_b^0 baryons. To probe the source of this inconsistency, the origins of both Λ_c^+ and Λ_b^0 baryons are analysed in conjunction with the initial conditions of heavy quarks preceding hadronisation. Understanding these initial quark states and the influence of hadronisation processes could provide valuable insights into baryon formation. Such investigations are essential for refining colour reconnection models and improving their consistency with experimental data across the full $p_\perp$ spectrum.

Acknowledgements

I would like to firstly acknowledge my supervisors, Peter Skands and Javira Altmann, for their exceptional guidance, encouragement, and expertise, which have profoundly shaped my development as a researcher. Their insights have been invaluable in advancing my understanding and skill in theoretical physics.

I would also like to thank Cooper Finnigan, who is my unofficial superhero. He has always provided advice regarding my research project, and has been willing to answer my questions when I felt lost. Cooper is truly a fantastic role model, and the best mentor an undergraduate physics student could ask for.

Finally, I would like to thank my friends, especially Sam, Bri, Connor, Steven and Kiril, who have offered support and encouragement countless times (and lots of c++ coding help).

Contents

1 Introduction

The production of heavy-flavour baryons in high-energy collisions at the Large Hadron Collider (LHC) offers a valuable insight into the fundamental interactions in Quantum Chromodynamics (QCD). In particular, this process occurs in the non-perturbative regime of QCD, where precise calculations become challenging. A key mechanism in this regime is colour reconnection, where coloured partons rearrange themselves to reduce the overall QCD string length. This reconnection process affects both the number of particles produced (particle yield) and their momentum characteristics. Recent improvements in colour reconnection models, which now incorporate a feature known as string junctions, have shown success in explaining charm baryon production [1]. For example, these models accurately predict the production ratio of the charm baryon Λ_c^+ to the meson D^0. The incorporation of string junctions suggests that baryons, unlike mesons, can be produced through the recombination of complex colour structures. This feature has brought theoretical predictions closer to experimental data, particularly in baryon-to-meson ratios.

Despite these advances, challenges remain in the case of bottom baryons. Although the Λ_c^+/D^0 ratio is well-described across different ranges of transverse momentum ($p_\perp$), the Λ_b^0/B^0 ratio shows significant discrepancies at low $p_\perp$. Models that incorporate string junctions in colour reconnection still fail to capture the observed behaviour of Λ_b^0 production at these low momenta. This discrepancy implies that some dynamics unique to bottom baryon production might be missing from current models.

In this study, these inconsistencies are investigated by analysing the origins of Λ_c^+ and Λ_b^0 baryons, with particular focus on the initial conditions of charm and bottom quarks prior to hadronisation. This analysis aims to identify any missing factors in colour reconnection models that could explain heavy-flavour baryon production at lower transverse momentums. A deeper understanding of these processes will refine QCD-based models, allowing for improved alignment between theoretical predictions and LHC data across all values of $p_\perp$.

2 Theory

2.1 Proton-Proton Collisions and the Large Hadron Collider

The Large Hadron Collider (LHC) is the world's highest-energy particle accelerator, located in Geneva, Switzerland. At CERN, the LHC facilitates proton-proton collisions, allowing detailed study of particle interactions. The ALICE and LHCb detectors are specifically designed for investigating heavy quarks and ions, particularly charm (c) and bottom (b) quarks. These quarks are produced in abundance during high-energy collisions, offering a unique opportunity to explore QCD and flavour physics. Understanding how quarks and gluons interact in these collisions provides insight into the fundamental structure of matter.

In a proton-proton collision, quarks and gluons—collectively known as partons—within the protons collide at high energies. These partons are held together by the strong force, mediated by gluons. When partons interact, the kinetic energy from the collision is transformed into new particles, which are typically not found in isolation under normal conditions. The energy of the collision initiates complex interactions, spanning both perturbative and non-perturbative regimes of QCD. This results in the creation of new particles, some examples being baryons (particles with 3 quarks) and mesons (particles with a quark and anti-quark). This provides a platform for studying the nature of quarks, gluons, and their interactions.

2.2 Monte Carlo Event Generators

Monte Carlo event generators are computational tools used to simulate particle collisions and the resulting interactions. These generators rely on random sampling techniques to model the probability distributions of various outcomes, mirroring those observed in nature [2]. In high-energy physics experiments like those conducted at the LHC, event generators play a critical role by bridging the gap between theoretical predictions and experimental results. They allow for the simulation of complex interactions, whilst providing a way to simulate millions of events with statistical accuracy. This enables both the testing of new theories and the optimisation of experimental designs.

One of the most widely used Monte Carlo event generators is Pythia, which is designed to simulate high-energy collisions between particles, such as those occurring at hadron colliders [2]. Pythia models each stage of a particle collision, from the initial hard scattering processes through to the final-state hadronisation. By incorporating both perturbative and non-perturbative QCD processes, Pythia provides a detailed picture of events, including phenomena such as particle decays and underlying event activities. In addition to Standard Model processes, Pythia can be customised to explore new physics scenarios, making it an invaluable tool for both experimental and theoretical particle physicists [2].

2.3 Hard and Soft Processes

Within Pythia, hard processes refer to interactions between partons at high momentum transfers [2]. These interactions are primarily responsible for producing high-energy final states, which are observed in collisions at the LHC. Hard processes are calculated using perturbative QCD, where the strong coupling constant is small enough to make the calculations tractable.

However, not all interactions occur at high momentum transfers. Soft processes involve lower-energy exchanges and cannot be easily described by perturbative QCD. To model these interactions, Pythia complements its hard scattering calculations with non-perturbative models, such as hadronisation, which describes the process by which partons form colour-neutral hadrons [2]. Pythia employs the Lund String Model to simulate hadronisation, ensuring that the final state of an event includes the formation of real, observable particles [3]. By combining hard and soft processes in a unified framework,

Pythia provides a comprehensive simulation of a particle collision, from the initial parton interactions to the final hadronic state.

2.4 Hadronisation and Fragmentation

Fragmentation is a crucial step in the evolution of a high-energy particle collision, describing how quarks and gluons produced in the collision transform into observable hadrons. Since partons cannot exist freely due to colour confinement, they undergo a process where they fragment into jets, collimated sprays of hadrons, which are aligned with the direction of the original parton [4]. During this process, colour-connected partons separate at high energies, forming a string system that stretches the confining potentials until they rupture. When the string breaks, a quark-antiquark pair is created at the break point [1]. This breaking of the string is referred to as fragmentation, and it continues until the energy becomes too low to sustain further fragmentation.

Hadronisation is the process through which quarks and gluons, produced during a collision (or by fragmentation), transition into observable particles. During hadronisation, the strong force between quarks and gluons causes them to form colour-neutral states. The final outcome is a state of primary hadrons, many of which are unstable and decay into secondary hadrons, which group together to form jets. This process of fragmentation is illustrated in Figure 1.

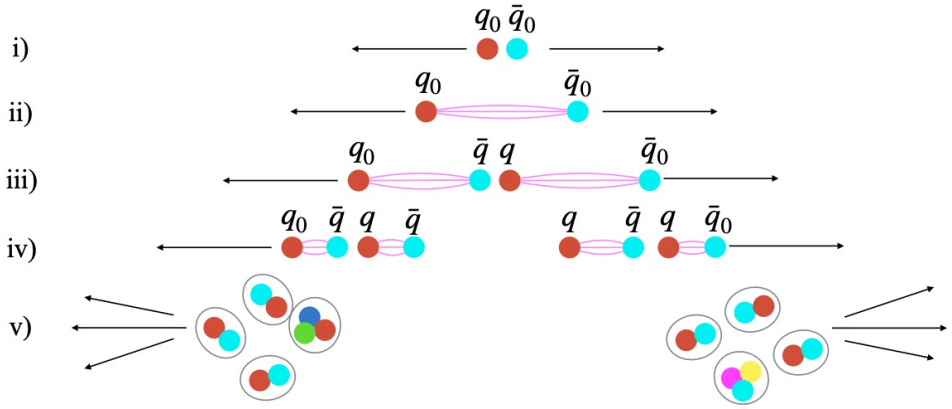

Figure 1: The process of hadronisation for a dipole string, where i) represents the quark antiquark ($q\bar{q}$) particles moving with high energy, ii) the string (colour flux tube) forming between the colour charged quark and antiquark, iii,iv) the string breaking and forming a new $q\bar{q}$ pairs, iv) hadronisation is complete, where colourless combinations of particles form jets [1].

Hadronisation plays a crucial role in the final stages of high-energy particle collisions, as it determines the types and distributions of the particles that emerge from the collision. However, because it occurs in the non-perturbative regime of QCD, where the strong coupling constant becomes large, hadronisation cannot be calculated directly from first principles. Instead, models like the Lund String Model are used to simulate the process [2].

The Lund String Model

The Lund String Model is the primary mechanism used by Pythia to model hadronisation [2]. In this model, when partons move apart, the strong force between them forms a colour field energy. This linear confinement potential is described by a "string" between static colour charges [5]. As the distance between the partons increases, the string stretches and eventually breaks, producing new quark-antiquark pairs that form hadrons.

2.5 String Topologies

Strings (colour flux tubes), are structures that form between partons to transmit the strong force. Dipole strings are a topology in which a string connects a quark anti-quark pair. The dipole string assists in describing the jet structure observed in high-energy collisions, where the momentum and spatial distribution of the hadrons reflects the dynamics of the original parton and its colour field.

In some cases, more complex topologies of strings can form, giving rise to junctions. In the Lund String Model, junction topologies are where three strings meet to form a "Y" shape. These junctions are particularly important for understanding the production of baryons. Junctions provide a mechanism for creating baryons during hadronisation, as they allow for the simultaneous confinement of three colour charges. This is a distinct feature in QCD that plays a significant role in particle collisions, and it can affect the baryon-to-meson ratio in the final state.

Figure 2: The left panel illustrates a quark-antiquark pair ($q\bar{q}$) with their respective colour charges (red and anti-red, represented as cyan), in a dipole string configuration. In the right panel, three quarks combine together in a junction configuration to create a colour neutral combination of quarks.

Junction Fragmentation and Baryon Production

Junctions are crucial in baryon production because they facilitate a fragmentation process where three quarks, each connected by a segment in a junction structure, combine to form baryons. In standard junction fragmentation, each leg of the junction is treated as half of a dipole string [6]. By boosting the system to the junction's rest frame, a fictitious leg is created for each junction leg, completing a full dipole string. This setup allows the hadronisation mechanism developed for dipole strings to be reused, effectively fragmenting the junction. This mechanism is demonstrated in Figure 3.

Figure 3: The left panel illustrates the two shortest legs of the junction forming the fictitious leg to complete the dipole. This allows for each of these respective legs to fragment as dipoles [1]. The right panel illustrates the fragmentation of the final leg, treated as a dipole. This forms a junction baryon, as demonstrated in the centre.

2.6 Colour Reconnection

Colour reconnection is an additional layer of complexity in the hadronisation process, where colour fields between partons interact and rearrange themselves before hadrons are formed. The process is thought to be mainly non-perturbative, occurring after the partons have undergone fragmentation but before hadronisation is complete. Colour reconnection can significantly alter the final distribution of hadrons, as it changes how partons are paired up to form colour-neutral particles.

Colour reconnection involves the rearrangement of colour charges in such a way that the energy stored in the colour strings between partons is minimised. This results in a more energetically favourable final state, where the momenta and types of the produced hadrons more closely resemble what is observed in nature.

Some examples of colour reconnection are demonstrated below, where the mechanism is demonstrated for producing mesons and baryons.

Figure 4: The left panel illustrates a configuration of two $q\bar{q}$ pairs with their respective colour charges (red and anti-red, represented as cyan). In the right panel, a more energetically favourable configuration is shown, which minimises the string length between $q\bar{q}$ pairs. Consequently, the quarks tend to reconnect in this configuration to fragment and form colour-neutral mesons.

Figure 5: The left panel illustrates a configuration of three $q\bar{q}$ pairs, each with unique colour charges. In the right panel, a more energetically favourable configuration is shown, which minimises the overall energy of the system. Consequently, the quarks will reconnect in a junction topology that will fragment to form colour-neutral baryons.

2.7 Baryon to Meson Ratio

In this study, the production ratios of Λ_c^+/D^0 and Λ_b^0/B^0 are examined, with Λ_c^+ composed of a c, u and d quark, and Λ_b^0 containing b, u and d quarks [7]. Additionally, the D^0 meson is composed of a c and $\bar{u}$ quark, whereas the B^0 meson is composed of a d and $\bar{b}$ quark [7]. Analysis shows that for the Λ_c^+/D^0 production ratio, the colour reconnection model effectively addresses differences between experimental and simulated results. This is further highlighted in Figure 6a. However, the model underperforms in predicting experimental outcomes for the Λ_b^0/B^0 ratio, especially at low transverse momentum values [1]. This is demonstrated in Figure 6b, where the colour reconnection model predicts twice the ratio observed in experimental results for low transverse momentum. This report investigates these differences to identify the underlying causes contributing to the divergence between simulated and experimental data.

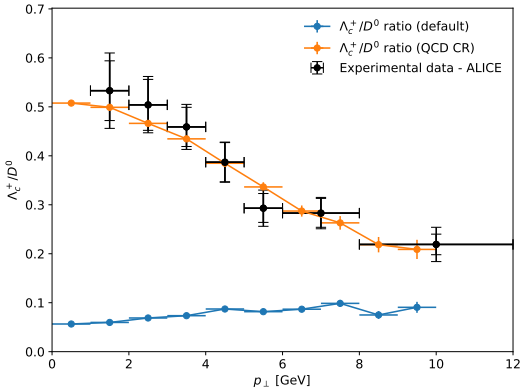

(a) Plot of the ratio of Λ_c^+/D^0 versus the transverse momentum to the beam axis. The experimental results (black) are from the ALICE collaboration [8], while simulated results from Pythia are shown without colour reconnection (blue) and with colour reconnection (orange). The experimental data spans the rapidity range $0 < y < 0.5$, and the Pythia simulations cover the rapidity range $|y| < 0.5$ for both configurations.

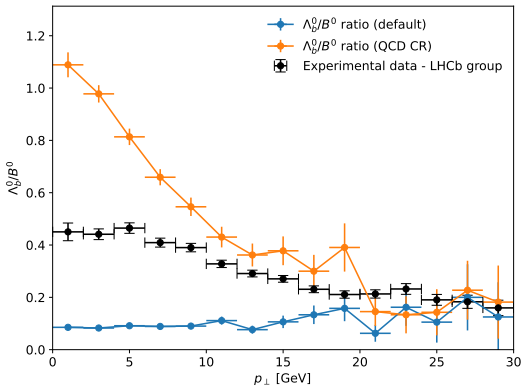

(b) Plot of the ratio of Λ_b^0/B^0 versus the transverse momentum to the beam axis. The experimental results (black) are from the LHCb collaboration [9], while simulated results from Pythia are shown without colour reconnection (blue) and with colour reconnection (orange). The experimental data spans the rapidity range $2 < y < 4.5$, while the Pythia simulations cover the rapidity ranges $2 < |y| < 4.5$ for both configurations.

Figure 6: The $p_\perp$ distributions of baryon-to-meson ratios are presented, with the left panel displaying the prompt Λ_c^+/D^0 ratio and the right panel showing the prompt Λ_b^0/B^0 ratio. Here, "prompt" refers to particles that originate directly from the primary interaction vertex, excluding those whose parent particles contain a b quark. All data were generated at a center-of-mass energy of $\sqrt{s} = 13$ TeV. The absolute value of the rapidity could be used in the results from Pythia, as the symmetry of the beam allows for the Monte Carlo statistics to be doubled [2].

To investigate the discrepancy in the baryon-to-meson ratio demonstrated in Figure 6b, the origin of the baryons is analysed. Investigating the production of baryons is crucial in understanding why the Λ_b^0/B^0 ratio diverges in simulated results compared to experimental observations at low transverse momentum values. Additionally, different experimental results that take pseudorapidity into account are compared to the colour reconnection model. Finally, the origin of c and b quarks in different string topologies is analysed to understand where these differences may arise in the simulation's production mechanisms.

3 Particle Production

Analysing the origin of the baryons in simulations can provide critical insight into the discrepancies in the predicted ratios of Λ_b^0/B^0 with colour reconnection effects. Status codes in Pythia simulations represent the production history and evolution of particles, allowing identification of whether a Λ_b^0 baryon originates directly from hadronisation, from decay chains, or in other manners [2]. By investigating the baryons' production mechanisms, it is possible to pinpoint where the simulation may diverge from experimental expectations, particularly if colour reconnection is influencing the hadronisation process differently than anticipated.

3.1 Results

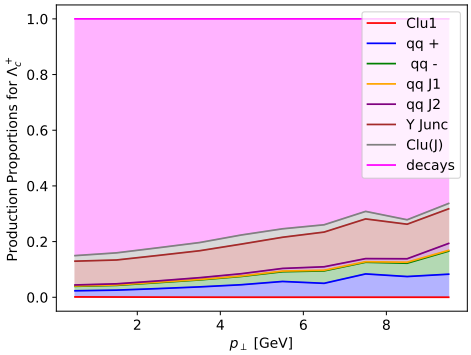

(a) Λ_c^+ baryon by origin.

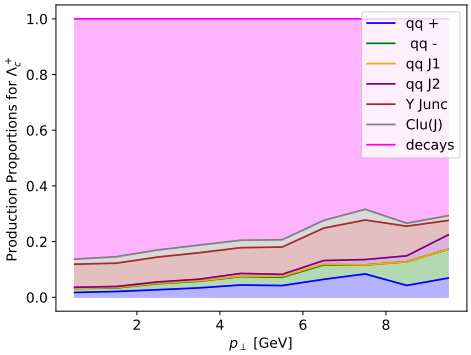

(b) Λ_c^+ baryon in the fiducial range $|y| < 0.5$ by origin

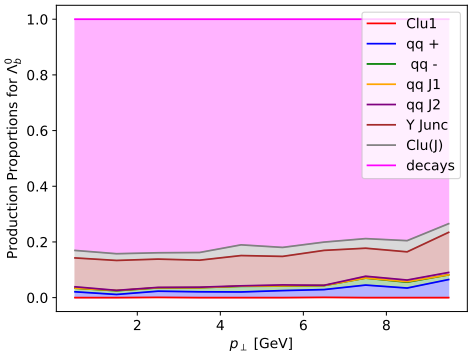

(c) Λ_b^0 baryon by origin

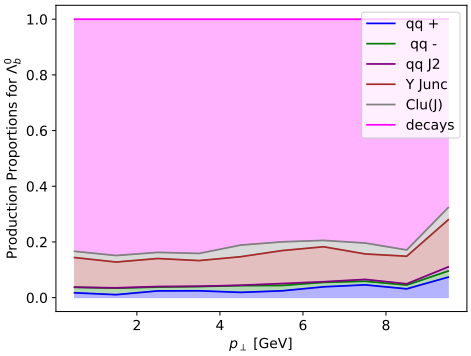

(d) Origin of in the the Λ_b^0 baryon in the fiducial range $2 < |y| < 4.5$ by origin

Figure 7: Origin of the Λ_c^+ baryon, implementing the colour reconnection model

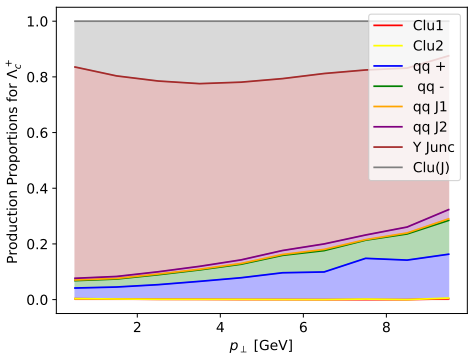

(a) Λ_c^+ baryon by origin of primary

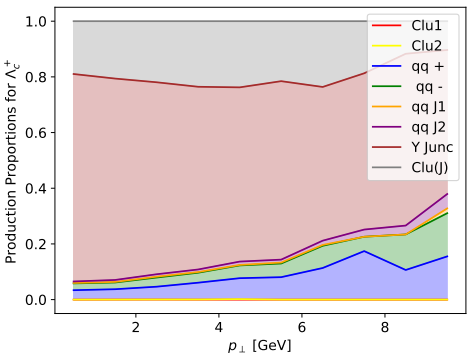

(b) Λ_c^+ baryon in the fiducial range $|y| < 0.5$ by origin of primary

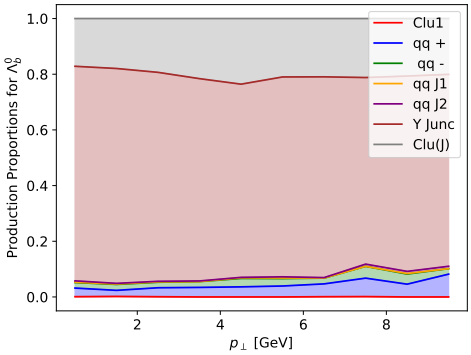

(c) Origin of the Λ_b^0 baryon, by origin of primary

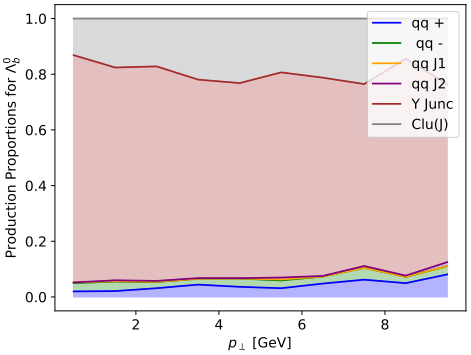

(d) Origin of the Λ_b^0 baryon in the fiducial range $2 < |y| < 4.5$ by origin of primary

Figure 8: Origin of the Λ_b^0 baryon, implementing the colour reconnection model

3.2 Discussion

3.2.1 Λ_c^+ Baryons by Origin

Figures 7a and 7b illustrate that, within the colour reconnection framework, a large proportion of Λ_c^+ baryons are produced via decays. At low transverse momentum, approximately 80% of these baryons originate from decays, regardless of their placement within the fiducial range of $|y| < 0.5$. The remaining 20% are formed through hadronisation processes, predominantly from junctions fragmenting. As transverse momentum increases, the contribution from decays decreases, with a greater share of baryons arising from dipole string fragmentation (shown in blue and green in Figures 7a and 7b). This shift occurs because higher transverse momentum allows for more energy in the system, thus favouring direct hadronisation mechanisms like dipole string fragmentation, which enhances the production of heavier baryons such as Λ_c^+ through direct fragmentation rather than secondary decays [10].

Within the fiducial range, the production proportions remain unchanged, maintaining the same distribution as observed in Figure 7a. Decay processes dominate at low transverse momentum, while hadronisation contributions increase with higher transverse momentum. This consistency highlights that the mechanisms influencing Λ_c^+ baryon production are inherent to the transverse momentum of particle creation rather than the kinematic constraints of the fiducial range. The fiducial cut primarily affects the rapidity distribution, but does not significantly alter the fundamental physics governing baryon production channels [11]. Consequently, the trend of decay dominance at low transverse momentum and increased hadronisation at high transverse momentum persists, driven more by energy-dependent fragmentation mechanisms than by rapidity constraints.

3.2.2 Λ_b^0 Baryons by Origin

Figures 7c and 7d reveal that a substantial portion of Λ_b^0 baryons are produced through decays. On average, about 80% of Λ_b^0 baryons originate from decay processes across all transverse momentum values, irrespective of their position within the fiducial range of $2 < |y| < 4.5$. The remaining 20% arise from hadronisation processes, primarily through junction fragmentation, suggesting a consistent decay mechanism dominating at these energy levels.

The dominance of decay contributions is attributed to the short lifetimes of the parent particles producing Λ_b^0 baryons, increasing the likelihood of decay before hadronisation occurs [7]. Additionally, the contribution from dipole interactions is relatively minor, as depicted by the green and blue regions in Figures 7c and 7d. This is largely because dipole emissions are more effective in producing lighter mesons than heavier baryons (such as those with a b quark), leading to an under-representation of baryon production in this channel [12].

Within the fiducial range defined as $2 < |y| < 4.5$, the proportions of Λ_b^0 baryon production remain consistent, with approximately 80% from decays and 20% from hadronisation processes. This consistency suggests that the fiducial range effectively captures the underlying dynamics of the collisions. The intrinsic properties governing the decay processes of Λ_b^0 baryons render them largely unaffected by the specific kinematic cuts imposed by the fiducial selection [7]. Furthermore, the extensive event statistics analysed help to minimise statistical fluctuations, ensuring that the production ratios reflect genuine physical processes rather than random variations. This stability across both regions supports the reliability of measurements and points to the processes governing baryon production being robust against rapidity variations.

3.2.3 Comparison of Baryons by Origin

Figure 7 demonstrates no visible difference in the production of baryons that could indicate the origin of the baryon-to-meson ratio. The proportions of baryon production at low transverse momentum

are consistent across each of the lambda baryons Λ_c^+ and Λ_b^0. This consistency suggests that the mechanisms governing baryon production are similar for both particle types within this momentum range.

3.2.4 Λ_c^+ Baryons Prior to Decaying

Figures 8a and 8b illustrates the production mechanisms of Λ_c^+ particles. Notably, when a baryon is produced through a decay process, the status of the primary hadron is considered in the analysis instead. These figures demonstrate that the production of Λ_c^+ baryons predominantly results from junction fragmentation (maroon). This underscores the significance of string dynamics in baryon formation, wherein the rearrangement of colour charges under strong interactions facilitates baryon production. Junctions serve as vital connections between quarks and antiquarks, with their fragmentation leading directly to baryon creation, particularly in high-energy collisions [2].

The distribution within the fiducial range (Figure 8b) remains similar to the distribution in Figure 8a, indicating that a baryon's origin is more closely tied to its energy rather than rapidity. As available energy increases, the likelihood of forming heavier baryons through junction and dipole fragmentation becomes more apparent, reflecting the interplay between particle properties, energy scales, and colour reconnection dynamics.

3.2.5 Λ_b^0 Baryons Prior to Decaying

Figures 8c and 8d illustrate the ratio of production mechanisms for the Λ_b^0 baryon, where any baryon from a decay has been re-categorised by the origin of the primary hardon. Additionally, the differences between 8c and 8d are minimal, which highlights that analysing particles within the fiducial range does not affect the origin of the Λ_b^0 particle. This consistency between the fiducial and non-fiducial data highlights that, for the Λ_b^0, the choice of fiducial cuts does not affect the production mechanism classification. Moreover, the increased mass of the Λ_b^0 baryon ($m_{\Lambda_b^0} = 5619.60 \pm 0.17$ MeV) [7] implies that it is predominantly produced in higher-energy environments, where production from junctions becomes significantly more probable than for its lighter counterpart Λ_c^+ ($m_{\Lambda_c^+} = 2286.46 \pm 0.14$ MeV) [7]. This difference emphasises the energy sensitivity of baryon production mechanisms, as well as the distinctive fragmentation processes between heavy and light baryons.

The observed predominance of junction topologies in Λ_b^0 production also suggests a potential threshold effect in the hadronisation process, where the mass of the b quark stabilises three-quark systems, making baryon formation more favourable at higher transverse momentum ranges. This effect could indicate that Λ_b^0 production is less sensitive to variations in initial quark kinematics, with the heavier quark promoting more frequent hadronisation in junction-dominated configurations.

3.2.6 Comparison of Baryons Prior to Decaying

Analysing Figure 8c and 8d, there are fewer Λ_b^0 baryons being produced by dipole strings in comparison to the Λ_c^+ ratios from Figures 8a and 8b. This is likely due to the increased mass of the Λ_b^0 baryon, which requires higher energy thresholds for direct production through dipole string fragmentation, making junction fragmentation the more favourable production mechanism at these energy scales [13].

Additionally, this tendency for junction-driven production of heavy baryons highlights an interesting contrast in the energy landscape required for baryon formation in heavy quark systems. Given that dipole fragmentation tends to favour mesons, the reduced dipole string production in Λ_c^+ and Λ_b^0 could be attributed to the energetically disfavoured nature of high-mass dipole configurations. This reliance on junction topologies for both Λ_c^+ and Λ_b^0 production could offer insights into the distinct fragmentation pathways followed by heavy quarks.

4 Semi-Leptonic Decays

To investigate the observed discrepancy in the production ratio of Λ_b^0/B^0, an additional dataset collected by the LHCb collaboration was compared to the colour reconnection model. This dataset, gathered in 2019, also included measurements of B^+ and B^- mesons. Assuming that the production of B^+ and B^- mesons is twice that of B^0 [14], these results can be directly compared to the more recent LHCb measurement from 2021. Furthermore, the 2019 LHCb dataset encompasses a pseudorapidity range of $2 < |\eta| < 5$, as illustrated in Figure 9b.

4.1 Results

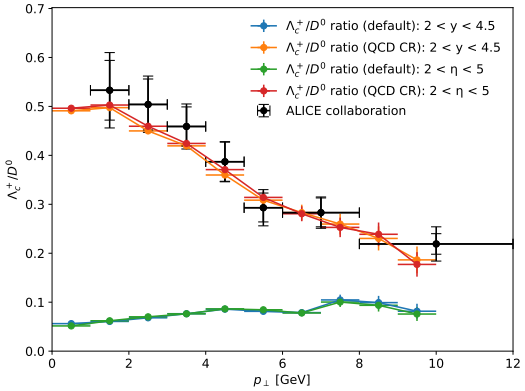

(a) The ratio of Λ_c^+/D^0 plotted against $p_\perp$, along with the rapidity restriction of $2 < |y| < 4.5$ for the Monash (2013) tune (blue), and colour reconnection model (orange). The pseudorapidity between $2 < \eta < 5$ is also shown with the default Monash tune (green) and colour reconnection model (red). The experimental results (black) are for rapidity in the range $y < 0.5$ [8].

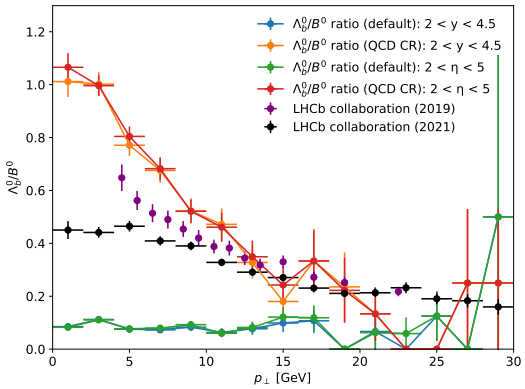

(b) The ratio of Λ_b^0/B^0 plotted against $p_\perp$, along with the rapidity restriction of $2 < |y| < 4.5$ for the Monash (2013) tune (blue), and colour reconnection model (orange). The pseudorapidity between $2 < |\eta| < 5$ is also shown with the default Monash tune (green) and colour reconnection model (red). The experimental results from the LHCb collaboration (black) are for rapidity in the range $2 < y < 4.5$ [9], and the second experimental data (purple) is from the 2019 LHCb collaboration [15] with pseudorapidity $2 < \eta < 5$.

Figure 9: The baryon to meson ratio demonstrating rapidity restrictions of $2 < |y| < 4.5$ and pseudorapidity restrictions of $2 < |\eta| < 5$ with the colour reconnection model.

4.2 Discussion

Figure 9a demonstrates that the colour reconnection model effectively describes the experimental results of the ratio Λ_c^+/D^0, even across varying rapidity and pseudorapidity ranges. This consistency indicates that the model's accuracy is largely unaffected by these different ranges, suggesting that the particle production mechanisms in the colour reconnection model are stable. Additionally, the minimal difference observed between models with rapidity versus pseudorapidity restrictions suggests that particle production remains uniform along the direction of the particle beam. This stability may result from the high-energy conditions modeled by Pythia, where the process of string fragmentation produces similar outcomes across different rapidity ranges.

Figure 9b demonstrates a comparable behaviour for the ratio of Λ_b^0/B^0, where the difference in the rapidity and pseudorapidity models is minimal. This observation implies that particle production is

largely uniform along the beam axis. Furthermore, the colour reconnection model provides a notably closer fit to the experimental data from the 2019 LHCb collaboration (purple) than to that from the 2021 LHCb collaboration (black). Although the 2021 collaboration concluded that these experimental results are in agreement [9], it is evident that the 2019 results align more closely with the colour reconnection model. To confirm these findings, additional data points at lower transverse momentum values would be beneficial.

In Figures 9a and 9b, at very low transverse momentum values (between 0 and 0.5 GeV), the baryon-to-meson ratio exhibits a plateau. This behaviour may arise from limitations in resolving distinct hadronisation processes in this momentum range. In this region, each heavy quark (c and b) lacks sufficient momentum to strongly differentiate between hadron types, resulting in a more uniform particle ratio.

5 String Topologies

Examining the initial-state properties of b and c quarks in different string configurations sheds light on how various production topologies impact baryon formation. Understanding these topologies is crucial, as they influence the dynamics of quark pair production and subsequent hadronisation processes, thereby influencing the baryon to meson ratio. Different string configurations can lead to varying colour flows and force interactions, which play a significant role in the formation of hadrons. By analysing these aspects, it becomes possible to identify potential systematic mismatches in the colour reconnection model's predictions for the ratio of baryons to mesons, which may contribute to the observed discrepancies.

5.1 Results

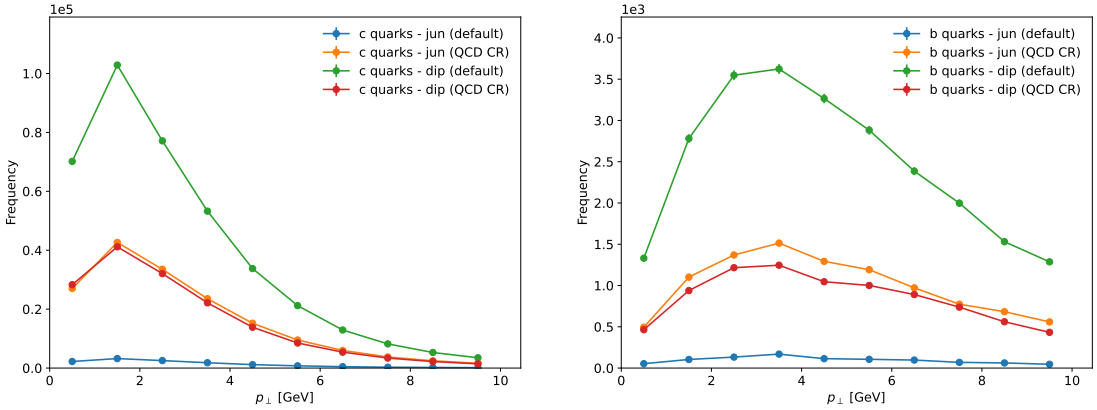

(a) Plot of $p_\perp$ of the c quark (before baryon or meson formation), categorised by their connection to either junction strings or dipole strings.

(b) Plot of $p_\perp$ of the b quark (before baryon or meson formation), categorised by their connection to either junction strings or dipole strings.

Figure 10: Distribution of the frequency of heavy quark against its transverse momentum, categorised by different topologies. The colour reconnection model is also considered to observe how this changes the ratio of quarks in junction or dipole topologies

5.2 Discussion

Within Figure 10, it is evident that both b and c quarks are significantly more likely to be part of dipole configurations than junction topologies when colour reconnection is absent. This is because, without colour reconnection, junction structures are relatively rare; their formation requires specific conditions where three strings meet, which is uncommon in typical event topologies dominated by dipole strings. In a dipole framework, quarks tend to pair with antiquarks to form meson-like structures due to the lower energy required and the direct colour connections available. Junction topologies, by contrast, generally represent a higher-energy configuration and are associated with baryon production, a less probable outcome in the absence of colour reconnection. Therefore, the initial preference for dipole string configurations reflects the natural tendency of the system to minimise energy through simpler quark-antiquark pairings, leaving junctions as rare, high-energy events when colour reconnection is not involved.

In the presence of colour reconnection, however, Figure 10 reveals unity in the frequency of c and b quarks found in dipole versus junction topologies, indicating that colour reconnection promotes a balance across both configurations. This balance suggests that for all transverse momentum values, the frequency of c quarks in a dipole configuration prior to fragmentation is comparable to that in a junction topology. Similarly, for b quarks, the colour reconnection mechanism ensures an approximate equivalency in the distribution of b quarks connected to dipole and junction topologies.

As discussed in Section 3, baryons are more likely to originate from junction topologies, while dipole strings predominantly yield mesons [16]. At lower transverse momentum values, an equal number of heavy quarks in both topologies implies a baryon-to-meson ratio close to unity. However, Figure 6 shows that this outcome is not entirely reflected in the experimental results. One plausible explanation for this discrepancy is that a significant portion of junctions involving c quarks do not lead to baryon formation, whereas junction topologies with b quarks have a higher likelihood of producing baryons upon string fragmentation.

This behaviour is likely a result of the mass differences between c and b quarks. The b quark, with a mass of 4.183 ± 0.007 GeV [7], has a lower velocity at equivalent transverse momenta compared to the c quark, which has a mass of 1.273 ± 0.005 GeV [7]. Consequently, the higher velocity of c quarks leads to more frequent string breakages occurring behind them, reducing the probability of baryon formation relative to b quarks in junction configurations. This difference highlights how quark mass and resulting kinematic factors can influence the fragmentation topology and subsequent particle composition.

6 Conclusion and Outlook

Ultimately, this investigation revealed that the large majority of heavy baryons in the colour reconnection framework originate from junction topologies. This is because junctions are a system with three quarks, making hadronisation with three quarks more accessible, and thus easier to create baryons from junctions.

By analysing the topologies associated with different heavy quarks, it was found that for all transverse momentum values among b and c quarks, there was an equal likelihood of the heavy quark being in a junction topology as in a dipole topology. Since string junctions more commonly produce baryons and dipole strings more commonly produce mesons during hadronisation, the expected baryon-to-meson ratio is one-to-one. This discrepancy in the colour reconnection model for the Λ_b^0/B^0 ratio likely arises from the larger mass of the b quark, which tends to create more baryons compared to c quark. With a lighter mass, the higher velocity of the c quark often causes the string to snap behind it, reducing the likelihood of baryon formation. By contrast, the heavier b quark is more likely to facilitate baryon formation, as its velocity will not be as high, meaning that the string will remain connected to the

junction. In comparison to the experimental results, the 2021 LHCb results suggest that the b quark should follow a similar mechanism to the c quark, where it is more likely that the string connected to the b quark should snap, reducing the production of Λ_b^0 baryons.

For further investigation, several avenues could be pursued. To definitively conclude whether the colour reconnection model sufficiently describes the ratio of Λ_b^0/B^0, more experimental results could be obtained at lower transverse momentum, and the discrepancy behind the 2019 and 2021 LHCb results can be investigated. Additionally, another avenue for further investigation would be to investigate the snapping behaviour of junction strings in both the c and b quark sector. One approach could be to quantify the rate at which junction strings snap without producing baryons across different pT ranges for both quark types, focusing especially on lower pT values where snapping seems more frequent in the c system than in the b system. By modeling these dynamics, it is possible to determine whether specific characteristics of the heavy quark (such as mass or momentum) systematically affect the likelihood of baryon formation, and how these effects influence overall particle production in different topologies. Finally, exploring the correlation between quark velocity and string snapping in dipole versus junction configurations could enhance our understanding of the mechanisms driving baryon and meson formation, potentially allowing for more accurate predictions of baryon yields across both quark sectors.

References

[1] J. Altmann and P. Skands. "String junctions revisited". In: *JHEP* 07 (2024), p. 238. 10.1007/JHEP07(2024)238. arXiv: 2404.12040 [hep-ph].

[2] C. Bierlich et al. "A comprehensive guide to the physics and usage of PYTHIA 8.3". In: *SciPost Phys. Codebases* (2022), p. 8. 10.21468/SciPostPhysCodeb.8.

[3] B. Andersson et al. "Parton Fragmentation and String Dynamics". In: *Phys. Rept.* 97 (1983), pp. 31–145. 10.1016/0370-1573(83)90080-7.

[4] A. Hayrapetyan et al. "Measurement of Energy Correlators inside Jets and Determination of the Strong Coupling". In: *Physical Review Letters* 133.7 (Aug. 2024). ISSN: 1079-7114. 10.1103/physrevlett.133.071903.

[5] G. S. Bali and K. Schilling. "Static quark-antiquark potential: Scaling behavior and finite-size effects in SU(3) lattice gauge theory". In: *Phys. Rev. D* 46 (6 Sept. 1992), pp. 2636–2646. 10.1103/PhysRevD.46.2636.

[6] T. Sjöstrand and P.Z. Skands. "Baryon number violation and string topologies". In: *Nuclear Physics B* 659.1–2 (May 2003), pp. 243–298. ISSN: 0550-3213. 10.1016/s0550-3213(03)00193-7.

[7] Particle Data Group. "Review of Particle Physics". In: *Progress of Theoretical and Experimental Physics* 2024.8 (2024), pp. 1–60. 10.1093/ptep/ptac082.

[8] S. Acharya et al. "Λ_c^+ production in pp and in p-Pb collisions at $\sqrt{s_{NN}}$=5.02 TeV". In: *Phys. Rev. C* 104.5 (2021), p. 054905. 10.1103/PhysRevC.104.054905. arXiv: 2011.06079 [nucl-ex].

[9] R. Aaij et al. "Enhanced Production of Λb0 Baryons in High-Multiplicity pp Collisions at s=13 TeV". In: *Phys. Rev. Lett.* 132.8 (2024), p. 081901. 10.1103/PhysRevLett.132.081901. arXiv: 2310.12278 [hep-ex].

[10] B. Andersson et al. "A Model for Low-pT Hadronic Reactions with Generalizations to Hadron-Nucleus and Nucleus-Nucleus Collisions". In: *Physics Reports* 97.2 (1983), pp. 31–145. 10.1016/0370-1573(83)90080-7.

[11] R. D. Field and R. P. Feynman. "Quark Elastic Scattering as a Source of High Transverse Momentum Mesons". In: *Physical Review D* 15.9 (1977), pp. 2590–2616. 10.1103/PhysRevD.15.2590.

[12] D. Griffiths. *Introduction to Elementary Particles*. 2nd. Hoboken, NJ: Wiley-VCH, 2018. ISBN: 978-3-527-41103-1.

[13] R. K. Ellis, W. J. Stirling, and B. R. Webber. *QCD and Collider Physics*. Cambridge Monographs on Particle Physics, Nuclear Physics and Cosmology. Cambridge University Press, 1996.

[14] R. Aaij et al. "Measurement of B meson production cross-sections in proton-proton collisions at $\sqrt{s}$ = 7 TeV". In: *Journal of High Energy Physics* 2013.8 (Aug. 2013). ISSN: 1029-8479. 10.1007/jhep08(2013)117. http://dx.doi.org/10.1007/JHEP08(2013)117.

[15] R. Aaij et al. "Measurement of b hadron fractions in 13 TeV pp collisions". In: *Phys. Rev. D* 100.3 (2019), p. 031102. 10.1103/PhysRevD.100.031102. arXiv: 1902.06794 [hep-ex].

[16] N. Lewis et al. "Search for baryon junctions in photonuclear processes and isobar collisions at RHIC". In: *The European Physical Journal C* 84.6 (June 2024). ISSN: 1434-6052. 10.1140/epjc/s10052-024-12834-2.

Appendix

The parameters used in the default model and colour reconnection model are listed in Table 1.

Parameter	**Default**	**QCD Colour Reconnection Model**
StringPT:sigma	0.335	0.335
StringZ:aLund	0.68	0.36
StringZ:bLund	0.98	0.56
StringZ:rFactC	1.5	1.5
StringFlav:mesonCvector	1.5	1.5
StringFlav:probStoUD	0.217	0.2
StringFlav:probQQtoQ	0.081	0.078
StringFlav:probQQ1toQQ0join	0.5, 0.7, 0.9, 1.0	0.5, 0.7, 0.9, 1.0
MultiPartonInteractions:pT0Ref	2.28	2.25
BeamRemnants:remnantMode	0	1
BeamRemnants:saturation	-	5
ColourReconnection:mode	0	1
ColourReconnection:allowDoubleJunRem	on	off
ColourReconnection:m0	-	0.3
ColourReconnection:allowJunctions	-	on
ColourReconnection:junctionCorrection	-	1.20
ColourReconnection:timeDilationMode	-	2
ColourReconnection:timeDilationPar	-	0.18
ColourReconnection:lambdaForm	0	0
StringFragmentation:pNormJunction	2	2
StringFragmentation:pearlFragmentation	off	off

Table 1: Model Parameters Used in This Paper [1]